Pair-instability mass loss for top-down compact object mass calculations

M. Renzo,[1,2] D. D. Hendriks,[3] L. A. C. van Son,[4,5,6] and R. Farmer[6]

[1]*Center for Computational Astrophysics, Flatiron Institute, New York, NY 10010, USA*
[2]*Department of Physics, Columbia University, New York, NY 10027, USA*
[3]*Department of Physics, University of Surrey, Guildford, GU2 7XH, Surrey, UK*
[4]*Center for Astrophysics | Harvard & Smithsonian,60 Garden St., Cambridge, MA 02138, USA*
[5]*Anton Pannekoek Institute for Astronomy, University of Amsterdam, Science Park 904, 1098XH Amsterdam, The Netherlands*
[6]*Max-Planck-Institut für Astrophysik, Karl-Schwarzschild-Straße 1, 85741 Garching, Germany*

ABSTRACT

Population synthesis relies on semi-analytic formulae to determine masses of compact objects from the (helium or carbon-oxygen) cores of collapsing stars. Such formulae are combined across mass ranges that span different explosion mechanisms, potentialy introducing artificial features in the compact object mass distribution. Such artifacts impair the interpretation of gravitational-wave observations. We propose a "top-down" remnant mass prescription where we remove mass from the star for each possible mass-loss mechanism, instead of relying on the fallback onto a "proto-compact-object" to get the final mass. For one of these mass-loss mechanisms, we fit the metallicity-dependent mass lost to pulsational-pair instability supernovae from numerical simulations. By imposing no mass loss in the absence of pulses, our approach recovers the existing compact object masses prescription at the low mass end and ensures continuity across the core-collapse/pulsational-pair-instability regime. Our remnant mass prescription can be extended to include other mass-loss mechanisms at the final collapse.

1. INTRODUCTION

Stellar and binary population synthesis calculations are necessary to predict event rates and population statistics of astrophysical phenomena, including those involving neutron stars (NS) and black holes (BH). Typically, at the end of the evolution (carbon depletion) the mass of the core is mapped to a compact object mass, using a $M_{\text{comp. obj}} \equiv M_{\text{comp. obj}}(M_{\text{core}})$ informed by core-collapse (CC) simulations (e.g., Fryer et al. 2012; Spera et al. 2015; Mandel & Müller 2020; Couch et al. 2020, see also Zapartas et al. 2021; Patton et al. 2021) and/or (pulsational) pair instability (PPI) simulations (e.g., Belczynski et al. 2016; Woosley 2017; Spera & Mapelli 2017; Stevenson et al. 2019; Marchant et al. 2019; Farmer et al. 2019; Breivik et al. 2020; Renzo et al. 2020b; Costa et al. 2021).

The most commonly adopted algorithms to obtain compact object masses in the CC regime are the "rapid" and "delayed" prescriptions of Fryer et al. (2012). In both cases, the compact object is built from the "bottom-up", starting from a proto-NS mass and adding the amount of fallback expected in the (possibly failed) explosion. However the proto-NS mass and information about the core structure relevant to decide the fallback are usually not available in population synthesis calcula-

tions (e.g., Patton & Sukhbold 2020). Instead the total final mass of the star is arguably easier to constrain in population synthesis models.

At the transition between CC and PPI (roughly at carbon-oxygen cores of $\sim 35\,M_\odot$, Woosley 2017; Marchant et al. 2019; Farmer et al. 2019; Renzo et al. 2020b; Costa et al. 2021), a mismatch between commonly adopted fitting formulae exists. These are at least partly caused by differences in the stellar structures used to design these algorithms and impair the interpretation of gravitational-wave data (as pointed out in Fig. 5 of van Son et al. 2021). While it is possible that the BH mass function is discontinuous at the onset of the PPI regime (e.g., Renzo et al. 2020c; Costa et al. 2021, Hendriks et al., in prep.), the location and amplitude of a putative discontinuity should not be governed by a mismatch between the fitting formulae from different stellar evolution models.

2. TOP-DOWN COMPACT OBJECT MASSES

In contrast with the "bottom up" approach of Fryer et al. (2012), we propose a "top-down" way to build the compact object masses $M_{\text{comp. obj}}$. Starting from the total stellar mass we remove the amount of mass lost due to all of the processes associated with the (possibly failed) explosion:

$$M_{\text{comp. obj}} = M_{\text{pre}-\text{CC}} - (\Delta M_{\text{SN}} + \Delta M_{\nu,\text{core}} + \Delta M_{\text{env}} + \Delta M_{\text{PPI}} + \cdots) \tag{1}$$

where all masses are in $M_\odot$ units, $M_{\text{pre}-\text{CC}}$ is the total mass at the onset of CC, and each term in the parenthesis corresponds to a potential mass-loss mechanism: ΔM_{SN} for the CC ejecta, $\Delta M_{\nu,\text{core}}$ the change in gravitational mass of the core due to the neutrino losses, ΔM_{env} the loss of the envelope due to the change in gravitational mass corresponding to $\Delta M_{\nu,\text{core}}$ that can occur even in red supergiant "failed" core-collapse (Nadezhin 1980; Lovegrove & Woosley 2013; Piro 2013; Fernández et al. 2018; Ivanov & Fernández 2021), and ΔM_{PPI} the pulsational mass loss due to pair-instability. Each term may further be a function of the progenitor stellar or binary properties, and may be theoretically or observationally informed (e.g., ΔM_{SN} could be derived from the light curves of a large sample of observed SNe). Eq. 1 can be further extended by adding additional mass-loss mechanisms in the parenthesis (e.g., disk winds).

In the CC regime the previous approach from Fryer et al. (2012) can be recovered by setting $\Delta M_{\text{SN}} + \Delta M_{\nu,\text{core}} = M_{\text{pre}-\text{CC}} - M_{\text{comp. obj}}^{\text{Fryer}+12}$, where the last term is the compact object mass as predicted by Fryer et al. (2012) and ignoring the other mass loss terms, such as ΔM_{PPI} and ΔM_{env}.

3. NEW FIT FOR PPI EJECTA

The top-down approach of Eq. 1, imposes $\Delta M_{\text{PPI}} = 0$ at the edge of the PPI regime, which produces a smooth BH mass distribution. We fit the metallicity-dependent naked helium core PPI simulations of Farmer et al. (2019) to obtain $\Delta M_{\text{PPI}} \equiv \Delta M_{\text{PPI}}(M_{\text{CO}}, Z)$ as a function of the carbon-oxygen core mass (Fig. 1). While the fit of Farmer et al. (2019) provides the remaining mass after PPI, this is only an estimate of the BH mass because of the the other mass loss processes that might occurr (e.g., Renzo et al. 2020b; Powell et al. 2021; Rahman et al. 2021). Our approach fits the mass removed by PPI only, which is what is directly computed in Farmer et al. (2019).

The dashed curves in each panel of Fig. 1 show the fit Eq. 2 for each metallicity computed in Farmer et al. (2019). We neglect the (weak) metallicity dependence

of the minimum core mass for PPI, and we fit the publicly available data for initial He core masses between $38 - 60\,M_\odot$. We emphasize that Farmer et al. (2019) only simulated helium cores. In the case of a star with a H-rich envelope which is still present at the onset of the pulsations and if it is both extended and red, it can be easily removed by the first pulse (Woosley 2017; Renzo et al. 2020b). Thus the H-rich mass of red supergiants should be added to the ΔM_{PPI} provided here. It is unclear what occurs in cases when the envelope is compact and blue (e.g., Di Carlo et al. 2019; Renzo et al. 2020a; Costa et al. 2021).
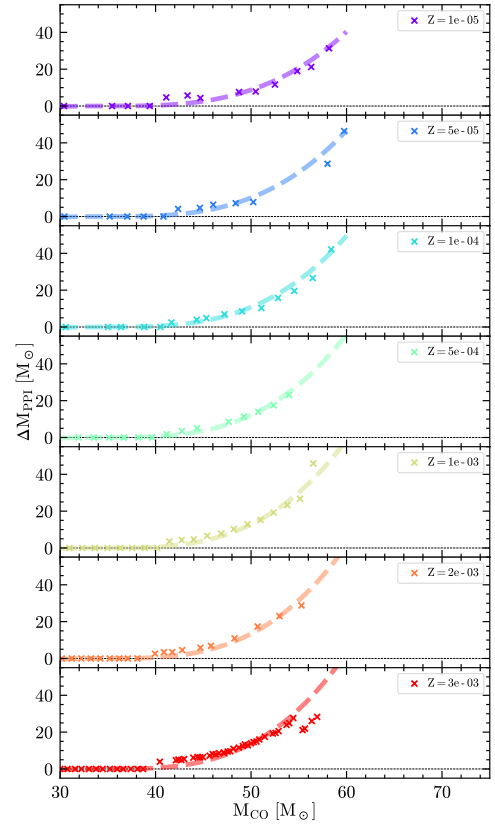

Figure 1. Each panel shows our fitting formula Eq. 2 for the amount of PPI induced mass-loss as a function of carbon-oxygen core mass at each metallicity Z as computed in Farmer et al. (2019). The crosses show the values from Tab. 1 Farmer et al. (2019).

$$\Delta M_{\text{PPI}} = (0.0006 \log_{10}(Z) + 0.0054) \times (M_{\text{CO}} - 34.8)^3 - 0.0013 \times (M_{\text{CO}} - 34.8)^2 \tag{2}$$

The amount of mass lost in PPI is sensitive to convection inside the star (Renzo et al. 2020c) and the assumed nuclear reaction rates (Farmer et al. 2019, 2020; Costa

et al. 2021; Woosley & Heger 2021; Mehta et al. 2021), which can introduce uncertainties up to $\sim 20\%$ on the maximum BH mass. The accuracy of our fit is comparable to these uncertainties.

ACKNOWLEDGEMENTS

REFERENCES

Belczynski, K., Heger, A., Gladysz, W., et al. 2016, A&A, 594, A97, doi: 10.1051/0004-6361/201628980

Breivik, K., Coughlin, S., Zevin, M., et al. 2020, ApJ, 898, 71, doi: 10.3847/1538-4357/ab9d85

Costa, G., Bressan, A., Mapelli, M., et al. 2021, MNRAS, 501, 4514, doi: 10.1093/mnras/staa3916

Couch, S. M., Warren, M. L., & O'Connor, E. P. 2020, ApJ, 890, 127, doi: 10.3847/1538-4357/ab609e

Di Carlo, U. N., Giacobbo, N., Mapelli, M., et al. 2019, MNRAS, 487, 2947, doi: 10.1093/mnras/stz1453

Farmer, R., Renzo, M., de Mink, S. E., Fishbach, M., & Justham, S. 2020, ApJL, 902, L36, doi: 10.3847/2041-8213/abbadd

Farmer, R., Renzo, M., de Mink, S. E., Marchant, P., & Justham, S. 2019, ApJ, 887, 53, doi: 10.3847/1538-4357/ab518b

Fernández, R., Quataert, E., Kashiyama, K., & Coughlin, E. R. 2018, MNRAS, 476, 2366, doi: 10.1093/mnras/sty306

Fryer, C. L., Belczynski, K., Wiktorowicz, G., et al. 2012, ApJ, 749, 91, doi: 10.1088/0004-637X/749/1/91

Ivanov, M., & Fernández, R. 2021, ApJ, 911, 6, doi: 10.3847/1538-4357/abe59e

Lovegrove, E., & Woosley, S. E. 2013, ApJ, 769, 109, doi: 10.1088/0004-637X/769/2/109

Luger, R., Bedell, M., Foreman-Mackey, D., et al. 2021, arXiv e-prints, arXiv:2110.06271. https://arxiv.org/abs/2110.06271

Mandel, I., & Müller, B. 2020, MNRAS, 499, 3214, doi: 10.1093/mnras/staa3043

Marchant, P., Renzo, M., Farmer, R., et al. 2019, ApJ, 882, 36, doi: 10.3847/1538-4357/ab3426

Mehta, A. K., Buonanno, A., Gair, J., et al. 2021, arXiv e-prints, arXiv:2105.06366. https://arxiv.org/abs/2105.06366

Nadezhin, D. K. 1980, Ap&SS, 69, 115, doi: 10.1007/BF00638971

Patton, R. A., & Sukhbold, T. 2020, MNRAS, 499, 2803, doi: 10.1093/mnras/staa3029

Patton, R. A., Sukhbold, T., & Eldridge, J. J. 2021, arXiv e-prints, arXiv:2106.05978. https://arxiv.org/abs/2106.05978

Piro, A. L. 2013, ApJL, 768, L14, doi: 10.1088/2041-8205/768/1/L14

Powell, J., Müller, B., & Heger, A. 2021, MNRAS, 503, 2108, doi: 10.1093/mnras/stab614

Rahman, N., Janka, H.-T., Stockinger, G., & Woosley, S. 2021, arXiv e-prints, arXiv:2112.09707. https://arxiv.org/abs/2112.09707

Renzo, M., Cantiello, M., Metzger, B. D., & Jiang, Y. F. 2020a, ApJL, 904, L13, doi: 10.3847/2041-8213/abc6a6

Renzo, M., Farmer, R., Justham, S., et al. 2020b, A&A, 640, A56, doi: 10.1051/0004-6361/202037710

Renzo, M., Farmer, R. J., Justham, S., et al. 2020c, MNRAS, 493, 4333, doi: 10.1093/mnras/staa549

Spera, M., & Mapelli, M. 2017, MNRAS, 470, 4739, doi: 10.1093/mnras/stx1576

Spera, M., Mapelli, M., & Bressan, A. 2015, MNRAS, 451, 4086, doi: 10.1093/mnras/stv1161

Stevenson, S., Sampson, M., Powell, J., et al. 2019, ApJ, 882, 121, doi: 10.3847/1538-4357/ab3981

van Son, L. A. C., de Mink, S. E., Callister, T., et al. 2021, arXiv e-prints, arXiv:2110.01634. https://arxiv.org/abs/2110.01634

Woosley, S. E. 2017, ApJ, 836, 244, doi: 10.3847/1538-4357/836/2/244

Woosley, S. E., & Heger, A. 2021, ApJL, 912, L31, doi: 10.3847/2041-8213/abf2c4

Zapartas, E., Renzo, M., Fragos, T., et al. 2021, arXiv e-prints, arXiv:2106.05228. https://arxiv.org/abs/2106.05228